

Signal-binding Specificity of the μ 4 Subunit of the Adaptor Protein Complex AP-4*

Received for publication, November 22, 2000
Published, JBC Papers in Press, January 3, 2001, DOI 10.1074/jbc.M010591200

Ruben C. Aguilar^{‡§}, Markus Boehm^{‡§¶}, Inna Gorshkova^{¶**}, Robert J. Crouch[¶],
Kazuhiro Tomita^{‡‡}, Takashi Saito^{‡‡}, Hiroshi Ohno^{§§}, and Juan S. Bonifacino^{¶¶¶}

From the [‡]Cell Biology and Metabolism Branch and the [¶]Laboratory of Molecular Genetics, NICHD, National Institutes of Health, Bethesda, Maryland 20892, the ^{‡‡}Department of Molecular Genetics, Chiba University Graduate School of Medicine, 1-8-1 Inohana, Chuo-ku, Chiba 260-8670, Japan, and the ^{§§}Division of Molecular Membrane Biology, Cancer Research Institute, Kanazawa University, 13-1 Takaramachi, Kanazawa 920-0934, Japan

The medium (μ) chains of the adaptor protein (AP) complexes AP-1, AP-2, and AP-3 recognize distinct subsets of tyrosine-based (YXX \emptyset) sorting signals found within the cytoplasmic domains of integral membrane proteins. Here, we describe the signal-binding specificity and affinity of the medium subunit μ 4 of the recently described adaptor protein complex AP-4. To elucidate the determinants of specificity, we screened a two-hybrid combinatorial peptide library using μ 4 as a selector protein. Statistical analyses of the results revealed that μ 4 prefers aspartic acid at position Y+1, proline or arginine at Y+2, and phenylalanine at Y-1 and Y+3 (\emptyset). In addition, we examined the interaction of μ 4 with naturally occurring YXX \emptyset signals by both two-hybrid and *in vitro* binding analyses. These experiments showed that μ 4 recognized the tyrosine signal from the human lysosomal protein LAMP-2, HTGYEQF. Using surface plasmon resonance measurements, we determined the apparent dissociation constant for the μ 4-YXX \emptyset interaction to be in the micromolar range. To gain insight into a possible role of AP-4 in intracellular trafficking, we constructed a Tac chimera bearing a μ 4-specific YXX \emptyset signal. This chimera was targeted to the endosomal-lysosomal system without being internalized from the plasma membrane.

Some and mediate intracellular sorting events. AP complexes are thought to participate in protein sorting by inducing the formation of coated vesicles as well as concentration of cargo molecules within the vesicles. Concentration of integral membrane proteins is mediated by direct interaction of the AP complexes with sorting signals present within the cytosolic tails of the proteins. Several types of cytosolic sorting signals have been described, the most common of which are referred to as “tyrosine-based” or “dileucine-based” depending on which residues are critical for activity (5, 6).

The four AP complexes have a similar structure and are composed of two large chains ($\alpha/\gamma/\delta/\epsilon$ and β 1–4, 90–130 kDa), a medium chain (μ 1–4, ~50 kDa), and a small chain (σ 1–4, ~20 kDa), each of which subserves a different function. Extensive analyses of the α chain of AP-2 have shown that it interacts, either directly or indirectly, with many regulators of coat assembly and/or vesicle formation (7). By analogy, the $\gamma/\delta/\epsilon$ chains are presumed to interact with other proteins that play similar regulatory roles. β 1, β 2, and β 3 interact with the scaffolding protein, clathrin (8–10). In addition, β 1 and β 2 have been found to bind a subset of dileucine-based sorting signals (11). The μ chains, on the other hand, function as recognition molecules for signals conforming to the YXX \emptyset consensus motif (Y is tyrosine, X is any amino acid, and \emptyset is leucine, isoleucine, phenylalanine, methionine, or valine) (12–20). The exact role of the σ chains is unknown, although σ 1 and σ 3 are required for the functional integrity of the AP-1 and AP-3 complexes, respectively (21, 22).

Our laboratory has been particularly interested in the role of the μ chains in signal recognition. We have previously demonstrated that μ 1 and μ 2 display a bipartite structure, with the amino-terminal one-third being involved in interactions with the corresponding β chains and the C-terminal two-thirds being involved in recognition of YXX \emptyset -type signals (23). X-ray crystallography revealed that the YXX \emptyset -binding domain of μ 2 consists of a banana-shaped all- β structure to which the signals bind in an extended conformation (19). The Tyr and \emptyset residues fit into hydrophobic pockets on this domain. Both crystallographic (19) and binding (13–18) studies have suggested that the identities of the \emptyset residue and the residues surrounding the critical Tyr residue are important determinants of the specificity of interaction. Although the subsets of YXX \emptyset signals recognized by μ 1, μ 2, and μ 3A overlap to a significant extent, each chain nonetheless exhibits certain preferences for residues neighboring the critical Tyr residue (14). For example, μ 1, μ 2, and μ 3A prefer Leu, Leu, and Ile residues at the \emptyset positions and neutral, basic, and acidic residues at the X positions, respectively. We have argued that these preferences alone are unlikely to account for the functional specificity of each AP

The heterotetrameric adaptor protein (AP)¹ complexes AP-1, AP-2, AP-3, and AP-4 are components of protein coats that associate with the cytosolic face of organelles of the secretory and endocytic pathways (reviewed in Refs. 1–4). AP-2 is associated with the plasma membrane and mediates rapid internalization of endocytic receptors, whereas AP-1, AP-3, and AP-4 are associated with the *trans*-Golgi network and/or endo-

* This work was supported in part by a grant-in-aid for scientific research from the Ministry of Education, Science, Sports, and Culture of Japan (to H. O. and T. S.). The costs of publication of this article were defrayed in part by the payment of page charges. This article must therefore be hereby marked “advertisement” in accordance with 18 U.S.C. Section 1734 solely to indicate this fact.

§ These authors contributed equally to this work.

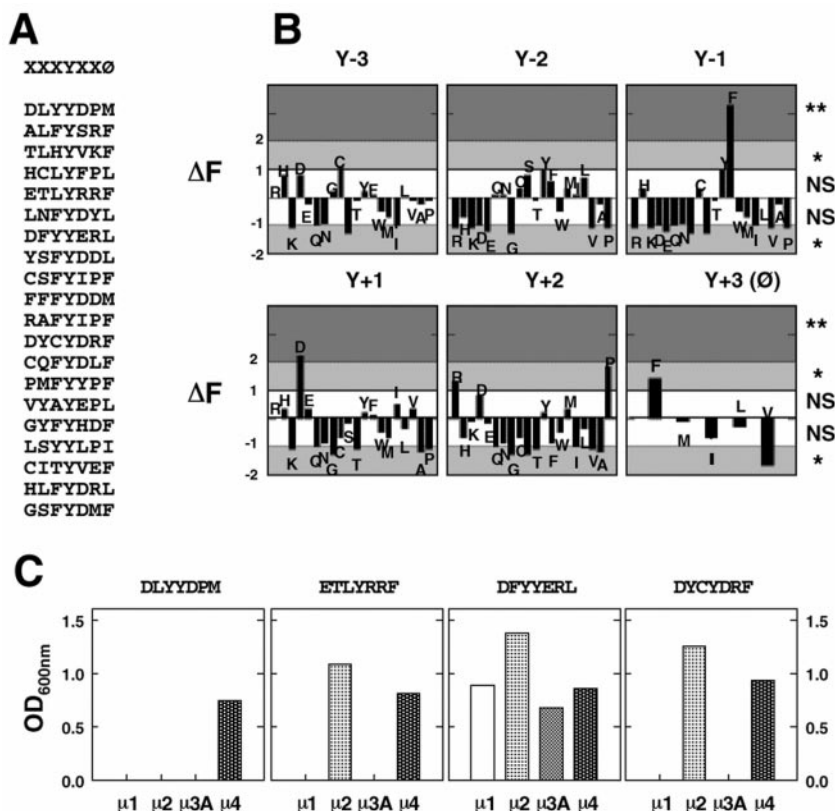
¶ Supported by a grant from the German Academic Exchange Service (DAAD).

** Supported by a National Research Council LMG-NICHD senior research associateship.

¶¶ To whom correspondence should be addressed: Cell Biology and Metabolism Branch, NICHD, Bldg. 18T, Rm. 101, NIH, Bethesda, MD 20892. Tel.: 301-496-6368; Fax: 301-402-0078; E-mail: juan@helix.nih.gov.

¹ The abbreviations used are: AP, adaptor protein; Gal4AD, Gal4 transcription activation domain; Gal4BD, Gal4 DNA-binding domain.

FIG. 1. Two-hybrid screening of a combinatorial peptide library. *A*, sequences of XXXYXX \emptyset clones selected by $\mu 4$. A Gal4BD-XXXYXX \emptyset library was co-expressed with a Gal4AD- $\mu 4$ construct in yeast cells. Co-transformants expressing interacting Gal4BD and Gal4AD constructs were selected in medium lacking tryptophan, leucine, and histidine and tested for expression of β -galactosidase activity. A list of the sequences obtained from library plasmids isolated from those clones is shown (see "Experimental Procedures" for details). *B*, statistical analysis of the library screening results. The preferences of $\mu 4$ for residues within the XXXYXX \emptyset sequence were inferred from the ΔF values in S.E. units (*y* axis; see "Experimental Procedures" for details) at each position (panels Y-3 to Y+3). Levels of significance are indicated by different gray tones, with the darkest representing the most significant (≥ 2 S.E. also indicated with **). NS, not significant. *C*, cross-reactivity analysis of some sequences selected by $\mu 4$. To test the binding specificity of signals selected by $\mu 4$ (indicated at the top of each panel), the corresponding Gal4BD constructs were co-transformed with different Gal4AD- μ constructs and tested for complementation of histidine auxotrophy. Cell growth in liquid medium lacking histidine was measured as turbidity at 600 nm.



complex (14). However, they probably contribute to the selectivity and efficiency of specific signal recognition events.

Although much has been done to characterize the signal-binding specificity of $\mu 1$, $\mu 2$, and $\mu 3A$, little is known about sequence preferences for the more recently described $\mu 4$ (also known as μ -AR $P2$) (24). Previous studies have shown that $\mu 4$ interacts weakly with YXX \emptyset signals from the lysosomal membrane proteins LAMP-1 (AGYQTI) (18) and CD63 (SGYEVM) (25) and the *trans*-Golgi network protein TGN38 (SDYQRL) (18). To determine whether $\mu 4$ might be able to recognize with higher affinity a defined subset of YXX \emptyset signals, we have undertaken a yeast two-hybrid screening of a combinatorial YXX \emptyset library. The results show that $\mu 4$ prefers signals with Phe at position Y-1, Asp at Y+1, Pro or Arg at Y+2, and Phe at Y+3 (\emptyset). A signal that fits this latter preference is found in the lysosomal membrane protein LAMP-2, and indeed, we found that the LAMP-2 signal binds to $\mu 4$ both in the yeast two-hybrid system and *in vitro*. We also found that a reporter integral membrane protein bearing a $\mu 4$ -specific YXX \emptyset signal is delivered to the endosomal-lysosomal system without being internalized from the plasma membrane.

EXPERIMENTAL PROCEDURES

Recombinant DNA Constructs—The constructs Gal4AD- $\mu 1$, Gal4AD- $\mu 2$, and Gal4AD- $\mu 3A$ in the pACTII(*LEU2*) plasmid (CLONTECH, Palo Alto, CA) have been described previously (12, 13). The Gal4AD- $\mu 4$ construct was prepared by ligating a *Bam*HI-*Sac*I polymerase chain reaction fragment corresponding to the 5'-part of $\mu 4$ and a *Sac*I-*Pst*I cDNA fragment corresponding to the 3'-part of $\mu 4$ into the *Bam*HI-*Xho*I sites of the pACTII(*LEU2*) vector using a *Pst*I-*Xho*I adaptor. As previously described (14), a DNA fragment encoding the 33-amino acid cytoplasmic tail of TGN38 engineered to contain an *Eag*I site (by introduction of silent mutations in place of the codons for Arg²¹ and Pro²² from the TGN38 cytoplasmic tail) was used to prepare the pGBT9-TGN Δ -*Eag*I construct by ligation into the *Eco*RI and *Xho*I sites of the pGBT9(*TRP1*) vector (CLONTECH). Oligonucleotides encoding either a combinatorial XXXYXX \emptyset peptide library (14) or different YXX \emptyset -type signals were digested with *Eag*I and *Pst*I and then ligated into pGBT9-TGN Δ -*Eag*I cut with *Eag*I and *Pst*I. The amino acid sequence encoded

by the resulting constructs was Gal4BD-HNKRKIIAFALEGKRSKVT-RRPKXXXYXX \emptyset . The construct Gal4BD- $\beta 2$ was kindly provided by Dr. M. S. Robinson (University of Cambridge, Cambridge, United Kingdom). All of the other two-hybrid constructs were made by ligation of polymerase chain reaction products into the pGBT9 or pACTII vector. The construct pET28a- $\mu 4$ -(156-453) was obtained by cloning nucleotides 466-1362 of the coding sequence of $\mu 4$ into pET28a (Invitrogen, Carlsbad, CA) using *Nhe*I and *Hind*III restriction sites. pET28a- $\mu 4$ -(156-453) was digested with *Nde*I and *Bst*EII to release a 1066-base pair fragment containing the amino-terminal His₆ tag and ligated with the *Nde*I-*Bst*EII fragment of vector pET16b (Invitrogen) containing the His₁₀ tag. The resulting construct was named pET28a-His₁₀- $\mu 4$ -(156-453). Interleukin-2 receptor α subunit (Tac) chimeric constructs were prepared by ligation of complementary oligonucleotides (coding for the PLSYTRF, DLYYDPM, and DLYADPM sequences) between an *Xba*I site inserted at the 3'-end of the Tac cDNA and the *Bam*HI site from the expression vector pCDL-SR α (26).

Yeast Culture, Transformation, and Two-hybrid Assays—The *Saccharomyces cerevisiae* strain HF7c (*MATa*, *ura3-52*, *HIS3-200*, *lys2-801*, *ade2-101*, *trp1-901*, *leu2-3,112*, *GAL4-542*, *gal80-538*, *LYS2::GAL1-HIS3*, *URA3::GAL4 17-mers*)3-*CYC1-lacZ*) (CLONTECH) was maintained on yeast extract/peptone/dextrose-agar plates. Transformations were done by the lithium acetate procedure as described in the instructions for the MATCHMAKER two-hybrid kit (CLONTECH). For colony growth assays, HF7c transformants were streaked on plates lacking leucine, tryptophan, and histidine and allowed to grow at 30 °C, usually for 4-5 days, until colonies were visible. For two-hybrid screening of the combinatorial library, the yeast cells were first transformed with Gal4AD- $\mu 4$ and plated onto yeast dropout agar plates lacking leucine as described in the protocol for the MATCHMAKER two-hybrid system. Transformants were re-transformed with the combinatorial DNA library and selected on plates lacking leucine and tryptophan for selection of co-transformants and lacking histidine for selection of interacting clones; Leu⁺Trp⁺ and His⁺ colonies were then tested for β -galactosidase activity. Colonies expressing β -galactosidase were cultured in dropout medium containing leucine but lacking tryptophan to obtain cells carrying only the library plasmid and not the medium subunit plasmid. The resulting cells were then mated with the yeast strain Y187 (*MATa*) transformed with Gal4AD- $\mu 4$ constructs or with pTD1-1 (SV40 large-T antigen cDNA in pACTII; negative control for histidine

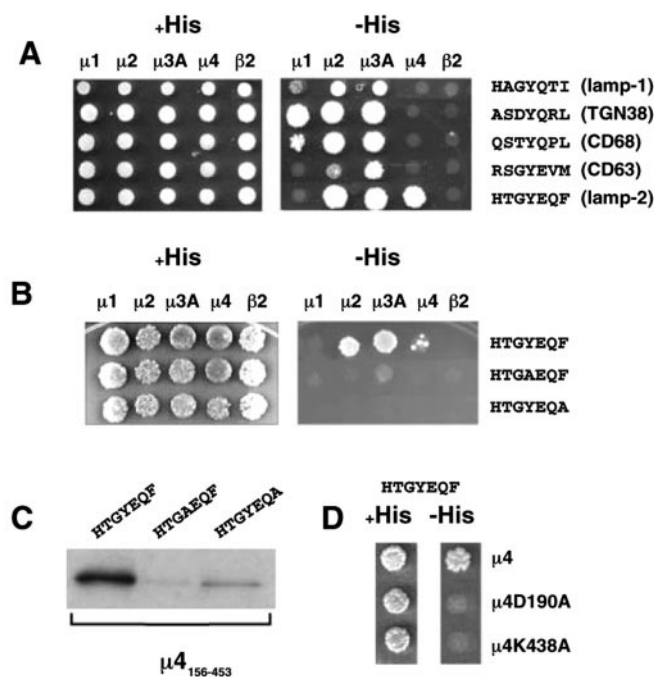


FIG. 2. Interaction of $\mu 4$ with the YXXØ signal from the lysosomal protein LAMP-2. *A*, analysis of the interaction of different μ chains with naturally occurring YXXØ-type signals. The source of each signal is indicated in parentheses. Yeast co-transformants expressing the Gal4AD-AP subunit and the Gal4BD signal constructs indicated were grown on plates lacking leucine and tryptophan, with or without histidine (+His and -His, respectively). *B*, yeast two-hybrid analysis of the interaction of AP chains with the LAMP-2 signal (HTGYEQF) and the HTGAEQF and HTGYEQA variants of this signal. *C*, *in vitro* binding of $\mu 4$ -(156–453) to the LAMP-2 signal (HTGYEQF) and the HTGAEQF and HTGYEQA variants of this signal. The biotinylated CWRKHHTGYEQF, CWRKHHTGAEQF, and CWRKHHTGYEQA peptides were bound to streptavidin-coated beads and incubated with *in vitro* transcribed/translated, radiolabeled $\mu 4$ -(156–453). *D*, analysis of the interaction of $\mu 4$ point mutants with the HTGYEQF signal. Mutants of $\mu 4$ carrying single amino acid substitutions of Asp¹⁹⁰ or Lys⁴³⁸ with Ala were examined for interaction with HTGYEQF using the yeast two-hybrid system.

auxotrophy and β -galactosidase activity) to test the binding specificity of library clones.

Cell Culture and Transfection—HeLa cells (American Type Culture Collection, Manassas, VA) were cultured in Dulbecco's modified Eagle's medium supplemented with 10% (v/v) fetal bovine serum, 100 units/ml penicillin, and 100 μ g/ml streptomycin (Biofluids, Inc., Rockville, MD) (regular medium). Primary cultures of skin fibroblasts from AP-3-deficient *mocha* mice (Jackson Laboratory, Bar Harbor, ME) were obtained as previously described (27) and maintained in regular medium. The night before transfection, cells were seeded onto 6-well plates (Costar Corp., Corning, NY) in 2 ml of regular medium. The following day, the cells were cotransfected with the Tac constructs and pCI-NEO (Promega, Madison, WI) using Fugene-6 reagent (Roche Molecular Biochemicals). To obtain stable transfectant clones, the regular medium from HeLa cells was replaced with fresh medium containing 1 mg/ml G418 (Calbiochem) 24 hours after transfection. The clones obtained were analyzed for expression of the Tac constructs by immunofluorescence microscopy.

Statistical Analyses—The experimental (observed) frequency for each residue at each position of the XXXYXXØ sequence was calculated using the sequences selected by the $\mu 4$ subunit from the combinatorial library. Preferences were evaluated by calculating the difference between the observed and expected frequencies (ΔF) in standard error units (14). Any ΔF value above 1 (*i.e.* favored) or below -1 (*i.e.* disfavored) was considered to be significantly different from 0 (random).

Site-directed Mutagenesis—Single amino acid substitutions were made using the QuickChange mutagenesis kit (Stratagene, La Jolla, CA). Briefly, 50 ng of plasmid carrying the target cDNA was incubated with two complementary primers (2 mM each) containing the desired mutation in the presence of 2 mM dNTP mixture and 2.5 units of *Pfu*

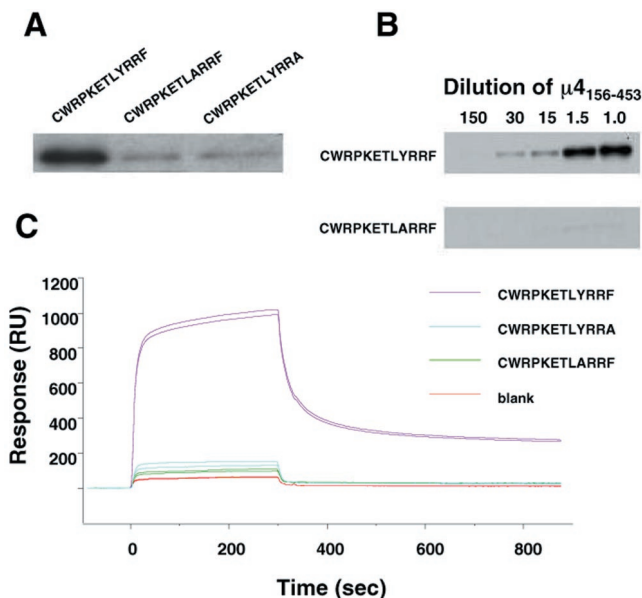


FIG. 3. Characterization of the interaction of the ETLYRRF sequence with recombinant $\mu 4$ -(156–453). The binding of $\mu 4$ -(156–453) to an ETLYRRF peptide, selected in the combinatorial screen (see Fig. 1C), was characterized using an *in vitro* binding assay (as described for Fig. 2C) and surface plasmon resonance spectroscopy. *A*, $\mu 4$ -(156–453) binds specifically to the ETLYRRF sequence and not to the Tyr-to-Ala or Phe-to-Ala variants of the sequence. *B*, concentration dependence of the binding of $\mu 4$ -(156–453) to the ETLYRRF peptide. Increasing amounts of $\mu 4$ -(156–453) were added to the biotinylated CWRPKETLYRRF and CWRPKETLARRF peptides bound to streptavidin beads. *C*, results from surface plasmon resonance experiments performed as described under "Experimental Procedures". $\mu 4$ -(156–453) (13.4 μ M) was injected onto streptavidin-coated flow cells previously loaded with the biotinylated CWRPKETLYRRF, CWRPKETLARRF, or CWRPKETLYRRA peptide. The results of two determinations for each peptide are shown. Notice that the binding of $\mu 4$ -(156–453) to ETLYRRF depends on the presence of the critical Tyr residue as well as the Phe residue at the Ø position. RU, response units.

DNA polymerase for 16 cycles according to the following temperature profile: 0.5 min at 95 °C, 1 min at 55 °C, and 8 or 16 min at 68 °C. After replication of both vector strands, the methylated parental DNA was digested for 1 h at 37 °C with 10 units of *DpnI* endonuclease, and the nicked vector with the desired mutation was transformed into *Escherichia coli*.

In Vitro Binding Assays—³⁵S-labeled $\mu 4$ -(156–453) protein was obtained by *in vitro* transcription/translation using the TNT T7 Quick coupled transcription/translation system (Promega) and Easytag™ expression protein labeling mixture (PerkinElmer Life Sciences) according to the manufacturers' instructions. In brief, 500 ng of the pET28a- $\mu 4$ -(156–453) construct was incubated with 20 μ l of TNT Quick Master Mix and 11 μ Ci of [³⁵S]methionine in a total volume of 25 μ l at 30 °C for 90 min. The transcription/translation reaction mixture (containing ³⁵S-labeled $\mu 4$ -(156–453)) was diluted 1:100 in binding buffer and centrifuged (180,000 \times g, 15 min, 4 °C). 500 μ l of supernatant was applied to peptide-coupled beads and incubated for 12 h at 4 °C. The beads were washed three times at 4 °C with binding buffer without bovine serum albumin, boiled in Laemmli sample buffer, and separated by SDS-polyacrylamide gel electrophoresis. The SDS gel was soaked in sodium salicylate and subjected to autoradiography.

Expression and Purification of $\mu 4$ -(156–453)—*E. coli* BL21(DE3) cells were transformed with pET28a-His₁₀- $\mu 4$ -(156–453); a single colony was picked; and the presence of the construct was verified. 2 liters of LB/kanamycin medium was inoculated with 100 ml of preculture and grown at 37 °C until A₆₀₀ reached 1.6. Protein expression then was induced by the addition of isopropyl- β -D-thiogalactopyranoside to a final concentration of 3 mM, and the cells were incubated at 37 °C for another 4 h. The cells were harvested, resuspended in buffer A (20 mM Tris-HCl (pH 8.0), 250 mM NaCl, and 5 mM imidazole), and sonicated. After centrifugation, the supernatant was loaded onto a Ni²⁺-nitrilotriacetic acid Superflow column (QIAGEN Inc., Valencia, CA), and the recombinant protein was eluted using buffer A with 1 M imidazole. $\mu 4$ -(156–453)-containing elution fractions were pooled; dialyzed

against 20 mM Tris-HCl (pH 7.0), 250 mM NaCl, 5 mM EDTA, and 0.5 mM dithiothreitol; and concentrated by centrifugation in a Centriprep-3 device (Amicon, Inc., Beverly, MA).

Preparation of Peptide-coupled Beads and Surface Plasmon Resonance Sensor Chips—The following peptides were obtained from Zymed Laboratories Inc. (South San Francisco, CA): CWKRHHTGYEQF, CWKRHHTGAEQF, CWKRHHTGYEQA, CWRPKETLYRRF, CWRPKETLARRF, and CWRPKETLYRRA. Peptide-coupled beads for *in vitro* binding assays were prepared by coupling the Cys residue of the peptides to EZ-Link™ PEO-maleimide-activated biotin (Pierce) in phosphate-buffered saline (pH 6.9) at peptide and biotin concentrations of 1 and 1.67 mM, respectively. The reaction was quenched by the addition of β -mercaptoethanol to a final concentration of 10 mM. 50 μ l of ImmunoPure immobilized streptavidin beads (Pierce) was washed twice with phosphate-buffered saline (pH 6.9), incubated overnight with 300 μ l of biotinylation reaction, and washed three times with binding buffer (0.05% (w/v) Triton X-100, 50 mM HEPES (pH 7.3), 10% (v/v) glycerol, 100 mM KCl, 2 mM MgCl₂, 0.1 mM CaCl₂, 50 μ M dithiothreitol, and 0.1% bovine serum albumin). Surface plasmon resonance experiments were carried out on a BIAcore 1000 instrument (BIAcore AB, Uppsala) at 25 °C using SA sensor chips with streptavidin covalently immobilized on a carboxymethylated dextran matrix. The chips were conditioned by 10 consecutive 1-min injections of 1 M NaCl, 50 mM NaOH, and 0.25% (w/v) SDS at a flow rate of 10 μ l/min and washed extensively with Tris-buffered saline (20 mM Tris-HCl (pH 7.0), 250 mM NaCl, 5 mM EDTA, and 0.005% (v/v) polysorbate 20). Biotinylated peptides were injected at a concentration of 500 nM in Tris-buffered saline running buffer at a flow rate of 2 μ l/min onto the chip surface until the desired level of immobilization (~150 response unit) was achieved. Unoccupied streptavidin was blocked by biotin (30 μ l of a 10 μ M solution at a flow rate of 5 μ l/min). The sensor chip was then washed by five consecutive 1-min injections of regeneration solution (25 mM NaOH, 500 mM NaCl, and 0.0005% (w/v) SDS). Flow cell 1 (with biotin-treated streptavidin) was left blank and used as a reference surface.

Surface Plasmon Resonance Spectroscopy—Surface plasmon resonance permits, in a label-free mode, real-time detection of binding events on the chip surface and estimation of binding parameters (28). 10 μ l of $\mu 4$ -(156–453) at the indicated concentrations was injected onto sensor chip surfaces. Dissociation of bound protein was carried out for 10 min, and then the surface was regenerated by two 30-s injections of regeneration solution and by two 30-s injections of running buffer. All experiments were repeated twice on two different chips. Data transformation and overlay sensorgrams were prepared using BIAevaluation Version 3.0 software (BIAcore AB). The response from the reference surface was subtracted from the other three flow cells to correct for refractive index changes, matrix effects, nonspecific binding, injection noise, and base-line drift. Using nonlinear least-squares fitting, the equilibrium dissociation constant (K_D) was evaluated by fitting data to a single site interaction model (Equation 1),

$$[RU_{eq}] = RU_{max}/1 + (K_D/C) \quad (\text{Eq. 1})$$

where RU_{eq} is the steady-state response level, RU_{max} is the maximal capacity of the surface (which was floated during the fitting procedure), and C is the concentration of $\mu 4$ in micromolar.

Antibodies and Immunofluorescence Microscopy—Immunofluorescence microscopy of fixed permeabilized cells and antibody internalization microscopy experiments were done as previously described (27, 29). The following monoclonal antibodies were used: anti-mouse LAMP-2 monoclonal antibody ABL-93, anti-human LAMP-2 monoclonal antibody H4B4, and anti-human CD63 monoclonal antibody H5C6 (Developmental Studies Hybridoma Bank, University of Iowa, Iowa City, IA). A polyclonal antiserum to recombinant Tac was raised in rabbits. Alexa 448 and Cy3-conjugated secondary antibodies were from Jackson ImmunoResearch Laboratories, Inc. (West Grove, PA).

RESULTS

Signal-binding Specificity of $\mu 4$ Determined by Screening of a Combinatorial XXXYXXXØ Yeast Two-hybrid Library—We have previously analyzed the signal-binding specificity of $\mu 1$, $\mu 2$, and $\mu 3$ (A and B isoforms) by screening a Gal4AD-XXXYYYXXXØ combinatorial library using the yeast two-hybrid system (14). Here, we have used the same method to define the signal-binding specificity of the $\mu 4$ subunit of AP-4. To this end, the combinatorial library was coexpressed with a Gal4AD- $\mu 4$ construct in yeast cells. Twenty clones that grew in medium

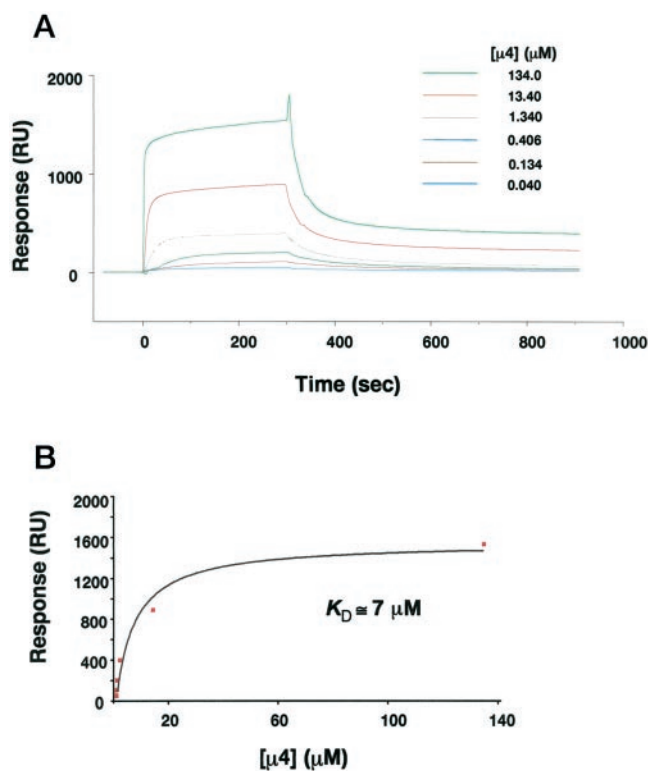


FIG. 4. Estimation of the affinity of the ETLYRRF sequence for $\mu 4$ -(156–453) by surface plasmon resonance spectroscopy. A, various concentrations of $\mu 4$ -(156–453) as indicated were injected onto streptavidin-coated flow cells previously loaded with the biotinylated CWRPKETLYRRF peptide. B, nonlinear least-squares fitting of the data shown in A yielded an equilibrium dissociation constant (K_D) of $7.0 \pm 2.5 \mu\text{M}$ for the binding of $\mu 4$ -(156–453) to the CWRPKETLYRRF peptide. RU, response units.

lacking histidine and that tested positive for β -galactosidase activity were isolated, and their amino acid sequences were deduced from DNA sequencing (Fig. 1A). A statistical analysis of the residues found at each position is shown in Fig. 1B; positive or negative ΔF values correspond to residues that were favored or disfavored, respectively. Only residues with ΔF values equal to or greater than 1 or equal to or lower than -1 were considered significant. Overall, $\mu 4$ seemed to have a distinct preference for aromatic amino acids at several positions of the XXXYXXXØ sequence. The most commonly found amino acids at each position were Cys, Tyr, Phe, Tyr, Asp, Pro, and Phe, respectively. Tyr was also favored at Y-1 and Arg at Y+2. Among the residues at the Ø position, the only preference was for Phe, whereas Val was strongly disfavored (Fig. 1B).

Some of the sequences selected by $\mu 4$ (DLYYDPM, ETLYRRF, DFYYERL, and DYC YDRF) were tested for their ability to interact with other μ subunits (Fig. 1C). The results showed that the DLYYDPM sequence was specific for $\mu 4$, whereas the ETLYRRF and DYC YDRF sequences interacted with $\mu 2$ and $\mu 4$, and the DFYYERL sequence interacted with all four μ chains (Fig. 1B). Thus, $\mu 4$ shares with the other μ chains the ability to interact with distinct but overlapping sets of YXXØ-type sequences.

Interaction of $\mu 4$ with Naturally Occurring Tyrosine-based Sorting Signals—To further characterize the interactions of $\mu 4$ with YXXØ motifs, we used the yeast two-hybrid system to test for interactions with YXXØ signals found in the cytosolic tails of some transmembrane proteins. The YXXØ signal of TGN38 was replaced by the analogous signals from LAMP-1, CD68, CD63, and LAMP-2, and interactions with μ chains were tested using the yeast two-hybrid system. A qualitative assay for

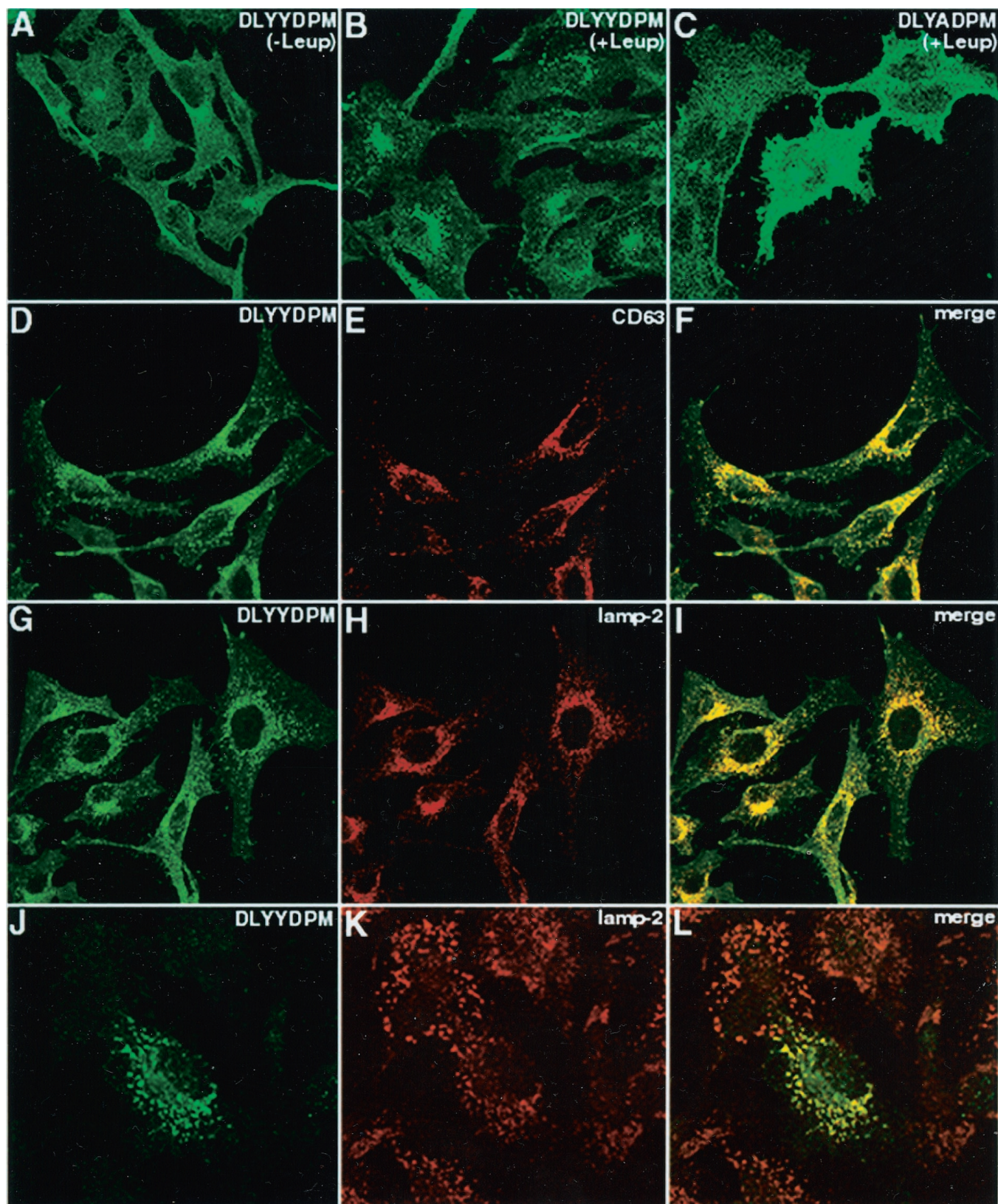


FIG. 5. **Intracellular distribution of a Tac chimera bearing a $\mu 4$ -specific signal.** A–I, HeLa cells stably transfected with a Tac-DLYYDPM chimeric construct were treated with (B–I) or without (A) leupeptin (*Leup*; 1 mg/ml) for 4 h. J–L, primary cultures of fibroblasts from AP-3-deficient *mocha* mice were transiently transfected with Tac-DLYYDPM. Fixed permeabilized cells were incubated with rabbit antiserum to the luminal domain of Tac and monoclonal antibodies to the lysosomal membrane proteins CD63 (D–F) and LAMP-2 (G–L), followed by incubation with Alexa 448-conjugated anti-rabbit and Cy3-conjugated anti-mouse IgG antibodies.

growth on histidine-deficient plates revealed that $\mu 4$ interacted only with the YXX \emptyset signal from human LAMP-2 (HTGYEQF) (Fig. 2A). The LAMP-2 signal was not recognized only by $\mu 4$

though, as it bound even more strongly to $\mu 2$ and $\mu 3A$ (Fig. 2, A and B). A salient feature of this signal is the presence of Phe at the \emptyset position, which fits the $\mu 4$ preferences deduced from

the combinatorial analyses. The Tyr-to-Ala and Phe-to-Ala variants of the LAMP-2 signal (HTGAEQF and HTGYEQA, respectively) were unable to interact with $\mu 4$ or with any other μ chain (Fig. 2B).

To verify the yeast two-hybrid results, we performed a binding assay using *in vitro* transcribed/translated $\mu 4$ -(156–453) and chemically synthesized and biotinylated LAMP-2 peptides. The peptides were bound to streptavidin beads and incubated with radioactively labeled $\mu 4$ -(156–453). Bound $\mu 4$ was revealed by SDS-polyacrylamide gel electrophoresis and fluorography. As shown in Fig. 2C, $\mu 4$ -(156–453) bound well to the wild-type LAMP-2 sequence (HTGYEQF), but only barely to the Tyr-to-Ala (HTGAEQF) and Phe-to-Ala (HTGYEQA) variants of the sequence.

The resolution of the crystal structure of the $\mu 2$ signal-binding domain allowed identification of residues that are directly involved in interactions with the critical tyrosine residue of the signals (19). Several of those residues are conserved in the other μ chains, including $\mu 4$ (3). To determine whether interactions of $\mu 4$ with YXX \emptyset signals involved conserved residues in the tyrosine-binding pocket, we mutated the conserved Asp¹⁹⁰ or Lys⁴³⁸ residue of $\mu 4$ to Ala. Two-hybrid assays revealed that these mutations abrogated interactions of $\mu 4$ with the tyrosine-based signal from LAMP-2 (Fig. 2D). Thus, the structural bases for the recognition of YXX \emptyset signals by $\mu 4$ appear to be similar to those of $\mu 2$.

Characterization of $\mu 4$ -YXX \emptyset Interactions by Surface Plasmon Resonance Spectroscopy— $\mu 4$ -YXX \emptyset interactions were further characterized by surface plasmon resonance spectroscopy. In these studies, we used three biotinylated peptides: CWRPKETLYRRF, corresponding to one of the sequences selected from the combinatorial library (Fig. 1B), and its Tyr-to-Ala (CWRPKETLARRF) and Phe-to-Ala (CWRPKETLYRRA) variants. Preliminary *in vitro* binding experiments showed that the CWRPKETLYRRF peptide bound radiolabeled $\mu 4$ -(156–453) (Fig. 3A) in a concentration-dependent manner (Fig. 3B), whereas CWRPKETLARRF and CWRPKETLYRRA did not (Fig. 3, A and B). The three biotinylated peptides were loaded onto separate flow cells of a streptavidin-coated chip. Recombinant $\mu 4$ -(156–453) was then applied, and binding of the protein was measured by an increase in response units. The signal for the CWRPKETLYRRF peptide at a concentration of 13.4 μM reached a plateau at ~ 1000 response units, whereas that of the two variant peptides only reached 100–150 response units. This was in the range of the nonspecific binding of $\mu 4$ -(156–453) to the biotinylated streptavidin surface without any peptide bound, as shown by the blank curve. After ending the injection of protein solution at 5 min, the value for the signal dropped sharply for all samples, indicating that the binding process was mostly reversible. However, $\sim 20\%$ of the binding could not be reversed even after washing for 10 min (data not shown). We performed an analysis of the interaction of different concentrations of $\mu 4$ -(156–453) with the CWRPKETLYRRF peptide (Fig. 4A). As expected, the signal amplitude was dependent on the amount of $\mu 4$ -(156–453) applied. The response approached a plateau value (a steady-state level, RU_{eq} (Equation 1)) after ~ 4.5 min. A plot of RU_{eq} against the concentration of $\mu 4$ is presented in Fig. 4B. Nonlinear regression analysis of these data yielded an apparent equilibrium dissociation constant of $7.0 \pm 2.5 \mu\text{M}$ and a maximum binding capacity (RU_{max}) of the surface of 1550 ± 165 response units. Although these values should be considered only estimates, it is nonetheless clear that the interactions are of low affinity.

Intracellular Localization of a Chimeric Protein Bearing a $\mu 4$ -specific Signal—To gain insights into the possible function of AP-4, we took advantage of the identification of a YXX \emptyset

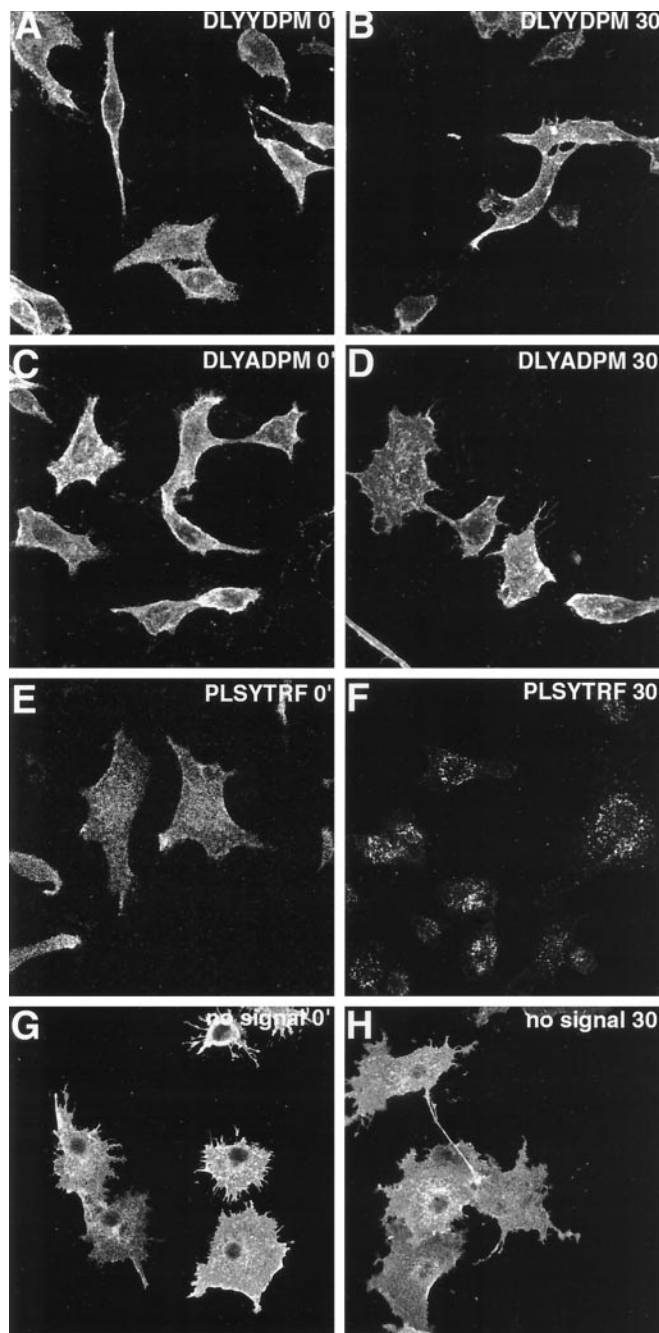


FIG. 6. Analysis of the internalization of Tac and Tac signal chimeras. Live HeLa cells stably expressing Tac (no signal) or Tac signal chimeras were incubated with anti-Tac antiserum for 1 h at 4 °C. After washing off the unbound antibody with phosphate-buffered saline, half of the cells were incubated at 37 °C for 30 min (B, D, F, and H) to allow antibody internalization, and the rest were kept at 4 °C as controls (A, C, E, and G). All the cells were then fixed, and the internalized antibody was detected by incubation with Cy3-conjugated anti-mouse IgG. The presence of the proteins at the plasma membrane was evidenced by staining of the outline of the cells (A–E and G–H), whereas internalized proteins were detected as intracellular vesicles (F).

signal (DLYYDPM) that was apparently specific for $\mu 4$ (Fig. 1B). This signal, as well as its corresponding Tyr-to-Ala mutant (DLYADPM), was appended to the cytosolic tail of the transmembrane protein Tac (29). The constructs were stably expressed in HeLa cells, and their intracellular distribution at steady state was examined by immunofluorescence microscopy using antibodies to the Tac luminal domain. We observed that the Tac-DLYYDPM chimera was present in the Golgi complex and plasma membrane (Fig. 5A). Treatment with the lysosomal

inhibitor leupeptin, however, resulted in accumulation of Tac-DLYYDPM in intracellular vesicles (Fig. 5B). Some of these vesicles colocalized with the lysosomal transmembrane proteins CD63 (Fig. 5, D–F) and LAMP-2 (Fig. 5, G–I), suggesting that a fraction of the Tac-DLYYDPM chimera was transported to late endosomes or lysosomes. The vesicular staining and colocalization of the chimera with LAMP-2 were not affected by the absence of the AP-3 complex in cells from the *mocha* mouse strain (Fig. 5, J–L) (30), consistent with the observation that the DLYYDPM signal does not interact with $\mu 3A$ (Fig. 1C). The DLYYDPM signal did not mediate internalization of the chimera from the cell surface (Fig. 6, A and B), whereas a PL-SYTRF signal derived from the transferrin receptor did (Fig. 6, E and F). As expected, the Tyr-to-Ala mutant chimera (DLY-ADPM) and a Tac construct without any tyrosine-based sorting signal were not significantly internalized (Fig. 6, C and D, and J and K, respectively). These observations were in agreement with the inability of the DLYYDPM signal to interact with $\mu 2$ and suggested that the vesicular localization of the Tac-DLYYDPM chimera was not the result of internalization from the cell surface.

DISCUSSION

The results of the experiments reported here show that $\mu 4$ shares, with other members of the μ family of AP subunits, the ability to recognize a subset of YXX \emptyset sorting signals. As is the case for other μ chains, interactions of $\mu 4$ with YXX \emptyset signals require the Tyr and \emptyset residues (Figs. 2 and 3) and are saturable (Fig. 4). These properties emphasize the remarkable structural conservation of the μ chain family of proteins. Indeed, of 15 residues in $\mu 2$ known to be involved in interactions with Tyr and \emptyset residues (19), 14 are identical in $\mu 4$ (3), with the remaining one being a conservative Leu¹⁷³ ($\mu 2$)-to-Val¹⁸⁷ ($\mu 4$) substitution. Mutation of one of two of the identical amino acids, Asp¹⁹⁰ or Lys⁴³⁸, to Ala abrogates interaction of $\mu 4$ with the signals (Fig. 2D), confirming that $\mu 2$ and $\mu 4$ recognize YXX \emptyset signals in a similar fashion.

These structural similarities notwithstanding, the subset of YXX \emptyset signals recognized by $\mu 4$ exhibits some characteristic features that distinguish it from that of other μ chains. The most salient feature of $\mu 4$ specificity is the preference for aromatic residues (Phe or Tyr) at various positions neighboring the critical Tyr residue. None of the other μ chains characterized to date exhibits this preference (14). The preference for Phe residues is particularly strong at the Y–1 and Y+3 (\emptyset) positions. In the case of the \emptyset position, this might be explained by the Leu¹⁷³ ($\mu 2$)-to-Val¹⁸⁷ ($\mu 4$) substitution. The smaller Val¹⁸⁷ residue lining the hydrophobic pocket could allow accommodation of the large aromatic side chain of Phe while disfavoring binding of the smaller Val side chain. Another preference specific for $\mu 4$ is Asp at position Y+1, whereas other preferences are similar to those of other μ chains. For instance, the selectivity for Pro at Y+2 appears to be a general characteristic of all the μ chains. This suggests that a bend in the polypeptide chain imposed by Pro stabilizes the conformation of the signals for interaction with μ chains. $\mu 4$ also favors Arg at Y+2, a preference shared only with $\mu 2$ (14). In the case of $\mu 2$, this preference for Arg is due to the establishment of hydrophobic interactions of the Arg side chain with Trp⁴²¹ and Ile⁴¹⁹ of $\mu 2$ and a hydrogen bond between the guanidinium group of Arg and Lys⁴²⁰ of $\mu 2$ (19). Two of these residues in $\mu 2$ (Trp⁴²¹ and Lys⁴²⁰) are conserved in $\mu 4$ (Trp⁴²⁹ and Lys⁴⁴⁰, respectively), but not in the other μ chains (3), which probably explains why only $\mu 2$ and $\mu 4$ favor Arg at Y+2.

Despite the fact that $\mu 4$ prefers certain residues at positions neighboring the critical Tyr residue, the subset of YXX \emptyset signals recognized by $\mu 4$ overlaps to a significant extent with

those recognized by other μ chains (Fig. 1C). This further strengthens the previous conclusion that μ chains recognize distinct but overlapping sets of YXX \emptyset signals (14). Therefore, the involvement of AP complexes in specific sorting events cannot depend solely on the specificity of signal recognition by their μ chains. Rather, the role of signal preferences is likely to “fine-tune” the efficiency of sorting.

A screening of several naturally occurring YXX \emptyset signals revealed that the lysosomal targeting signal from LAMP-2 (HTGYEQF) (30) interacts with $\mu 4$ (Fig. 2). This signal has a Phe residue at the \emptyset position, which could explain why it binds to $\mu 4$ (Fig. 1B). Previous studies had demonstrated weak interactions of $\mu 4$ with two other lysosomal membrane proteins, LAMP-1 (18) and CD63 (25). Taken together, these observations suggest a possible role for the AP-4 complex in sorting to lysosomes. However, the signals from all of these lysosomal membrane proteins interact better with $\mu 2$ and $\mu 3A$ than with $\mu 4$ (Fig. 2, A and B). To gain insight into the potential function of AP-4, we took advantage of the identification of a signal (DLYYDPM) that interacts exclusively with $\mu 4$ (Fig. 1C). This signal was placed at the cytosolic carboxyl terminus of a Tac chimeric construct devoid of other sorting signals (13). The resulting Tac-DLYYDPM chimera was expressed by stable transfection into HeLa cells, and its localization was determined by indirect immunofluorescence microscopy. In the absence of protease inhibitors, the protein exhibited a steady-state localization to the Golgi complex and plasma membrane. However, incubation with the lysosomal inhibitor leupeptin resulted in accumulation of the protein in lysosomes, as shown by colocalization with LAMP-2 (Fig. 5). This indicated that the Tac-DLYYDPM chimera is transported to and degraded in lysosomes. As expected, this accumulation was dependent on the critical Tyr residue of the signal. The Tac-DLYYDPM chimera was not efficiently internalized from the plasma membrane (Fig. 6), in accordance with its inability to interact with $\mu 2$ (Fig. 1C). In addition, the Tac-DLYYDPM chimera was still targeted to lysosomes in AP-3-deficient *mocha* cells, further demonstrating that AP-3 does not play a role in the recognition of the DLYYDPM signal. Even though our two-hybrid results indicated that there is no interaction between the DLYYDPM signal and $\mu 1$ (Fig. 1C), we cannot rule out the possibility that AP-1 could somehow be involved in sorting of the Tac-DLYYDPM chimera. However, Meyer *et al.* (31) have suggested that targeting of proteins to lysosomes is not affected in $\mu 1$ -deficient cells. These observations are consistent with the possibility that $\mu 4$ and, by extension, the AP-4 complex are involved in targeting proteins from the *trans*-Golgi network to the endosomal-lysosomal system. This involvement could provide an alternative means of sorting proteins to lysosomes, the existence of which has been suggested by previous studies (31–34). The evidence for a role of AP-4 in targeting to the endosomal-lysosomal system presented here, however, is indirect and should be considered tentative until it becomes possible to study protein sorting in AP-4-deficient cells. Attempts to ablate expression of this complex in mice are underway.

REFERENCES

- Lewin, D. A., and Mellman, I. (1998) *Biochim. Biophys. Acta* **1401**, 129–145
- Hirst, J., and Robinson, M. S. (1998) *Biochim. Biophys. Acta* **1404**, 173–193
- Bonifacino, J. S., and Dell’Angelica, E. C. (1999) *J. Cell Biol.* **145**, 923–926
- Kirchhausen, T. (1999) *Annu. Rev. Cell Dev. Biol.* **15**, 705–732
- Marks, M. S., Ohno, H., Kirchhausen, T., and Bonifacino, J. S. (1997) *Trends Cell Biol.* **7**, 124–128
- Bonifacino, J. S., Marks, M. S., Ohno, H., and Kirchhausen, T. (1996) *Proc. Assoc. Am. Physicians* **108**, 285–295
- Owen, D. J., and Luzio, J. P. (2000) *Curr. Opin. Cell Biol.* **12**, 467–474
- Gallusser, A., and Kirchhausen, T. (1993) *EMBO J.* **12**, 5237–5244
- Shih, W., Gallusser, A., and Kirchhausen, T. (1995) *J. Biol. Chem.* **270**, 31083–31090
- Dell’Angelica, E. C., Klumperman, J., Stoorvogel, W., and Bonifacino, J. S. (1998) *Science* **280**, 431–434

11. Rapoport, I., Chen, Y. C., Cupers, P., Shoelson, S. E., and Kirchhausen, T. (1998) *EMBO J.* **17**, 2148–2155
12. Ohno, H., Stewart, J., Fournier, M. C., Bosshart, H., Rhee, I., Miyatake, S., Saito, T., Gallusser, A., Kirchhausen, T., and Bonifacino, J. S. (1995) *Science* **269**, 1872–1875
13. Ohno, H., Fournier, M. C., Poy, G., and Bonifacino, J. S. (1996) *J. Biol. Chem.* **271**, 29009–29015
14. Ohno, H., Aguilar, R. C., Yeh, D., Taura, D., Saito, T., and Bonifacino, J. S. (1998) *J. Biol. Chem.* **273**, 25915–25921
15. Ohno, H., Tomemori, T., Nakatsu, F., Okazaki, Y., Aguilar, R. C., Foelsch, H., Mellman, I., Saito, T., Shirasawa, T., and Bonifacino, J. S. (1999) *FEBS Lett.* **449**, 215–220
16. Boll, W., Ohno, H., Songyang, Z., Rapoport, I., Cantley, L. C., Bonifacino, J. S., and Kirchhausen, T. (1996) *EMBO J.* **15**, 5789–5795
17. Stephens, D. J., Crump, C. M., Clarke, A. R., and Banting, G. (1997) *J. Biol. Chem.* **272**, 14104–14109
18. Stephens, D. J., and Banting, G. (1998) *Biochem. J.* **335**, 567–572
19. Owen, D. J., and Evans, P. R. (1998) *Science* **282**, 1327–1332
20. Storch, S., and Braulke, T. (2001) *J. Biol. Chem.* **276**, 4298–4303
21. Shim, J., Sternberg, P. W., and Lee, J. (2000) *Mol. Biol. Cell* **11**, 2743–2756
22. Mullins, C., Hartnell, L. M., and Bonifacino, J. S. (2000) *Mol. Gen. Genet.* **263**, 1003–1014
23. Aguilar, R. C., Ohno, H., Roche, K. C., and Bonifacino, J. S. (1997) *J. Biol. Chem.* **272**, 2760–2766
24. Wang, X., and Kilman, M. W. (1997) *FEBS Lett.* **402**, 57–61
25. Hirst, J., Bright, N. A., Rous, B., and Robinson, M. S. (1999) *Mol. Biol. Cell* **10**, 2787–2802
26. Takebe, Y., Seiki, M., Fujisawa, J., Hoy, P., Yokota, K., Arai, K., Yoshida, M., and Arai, N. (1988) *Mol. Cell. Biol.* **8**, 466–472
27. Dell'Angelica, E. C., Aguilar, R. C., Wolins, N., Hazelwood, S., Gahl, W. A., and Bonifacino, J. S. (2000) *J. Biol. Chem.* **275**, 1300–1308
28. Jonsson, U., Fagerstam, L., Ivarsson, B., Johnsson, B., Karlsson, R., Lundh, K., Lofas, S., Persson, B., Roos, H., Ronnberg, I., Sjolander, S., Stenberg, E., Stahlberg, R., Urbaniczky, C., Ostlin, H., and Malmqvist, M. (1991) *BioTechniques* **11**, 620–627
29. Humphrey, J. S., Peters, P. J., Yuan, L. C., and Bonifacino, J. S. (1993) *J. Cell Biol.* **120**, 1123–1135
30. Kantheti, P., Qiao, X., Diaz, M. E., Peden, A. A., Meyer, G. E., Carskadon, S. L., Kapfhamer, D., Sufalko, D., Robinson, M. S., Noebels, J. L., and Burmeister, M. (1998) *Neuron* **21**, 111–122
31. Meyer, C., Zizioli, D., Lausmann, S., Eskelinen, E. L., Hamann, J., Saftig, P., von Figura, K., and Schu, P. (2000) *EMBO J.* **19**, 2193–2203F. K.
32. Le Borgne, R., Alconada, A., Bauer, U., and Hoflack, B. (1998) *J. Biol. Chem.* **273**, 29451–29461
33. Feng, L., Seymour, A. B., Jiang, S., To, A., Peden, A. A., Novak, E. K., Zhen, L., Rusiniak, M. E., Eicher, E. M., Robinson, M. S., Gorin, M. B., and Swank, R. T. (1999) *Hum. Mol. Genet.* **8**, 323–330
34. Dell'Angelica, E. C., Shotelersuk, V., Aguilar, R. C., Gahl, W. A., and Bonifacino, J. S. (1999) *Mol. Cell* **3**, 11–21